Available online at www.sciencedirect.com
ScienceDirect
Journal of Solid State Chemistry 180 (2007) 3504–3509
JOURNAL OF SOLID STATE CHEMISTRY
www.elsevier.com/locate/jssc

Zirconium tungstate hydroxide hydrate revisited: Crystallization dependence on halide and hydronium ions

Julie A. Colin[1], DeMarco V. Camper, Stacy D. Gates, Monty D. Simon[2], Karen L. Witker[3], Cora Lind*

Department of Chemistry, MS 602, The University of Toledo, Toledo, OH 43606, USA

Received 1 August 2007; received in revised form 12 October 2007; accepted 14 October 2007
Available online 22 October 2007

Abstract

The formation of zirconium tungstate hydroxide hydrate, a precursor to the negative thermal expansion material cubic zirconium tungstate, shows a strong dependence on hydrothermal reaction conditions. It was found that not only the acid concentration, but also the acid counterion plays a significant role in the crystallization of $ZrW_2O_7(OH)_2 \cdot 2H_2O$. High temperatures, high acid concentrations, and the presence of chloride or bromide ions promote the formation of well-crystallized $ZrW_2O_7(OH)_2 \cdot 2H_2O$. For low acid concentrations, a new zirconium tungstate hydrate polymorph is observed, which transforms to tetragonal $ZrW_2O_7(OH)_2 \cdot 2H_2O$ at longer reaction times. A study of crystallization kinetics in hydrochloric acid is presented.

Keywords: Zirconium tungstate hydroxide hydrate; Crystallization; Hydrothermal; Kinetics; New polymorph

1. Introduction

Negative thermal expansion (NTE) materials have been of great interest over the last decade [1–9]. While most materials expand with increasing temperature, NTE materials contract upon heating. This makes them attractive as fillers for use in composites, where they can counteract the positive thermal expansion of the matrix material [10–15]. Among the most promising materials for this type of application is the cubic AM_2O_8 family (A = Zr, Hf; M = Mo, W), which undergoes isotropic NTE over a large temperature range [16–18]. Another advantage is that these compounds can be prepared from inexpensive, commercially available starting materials.

At room temperature, all compounds in the cubic AM_2O_8 family are metastable with respect to their constituent binary oxides [19]. The tungstates are thermodynamically stable at high temperatures [20], and can be prepared by traditional solid-state reactions followed by quenching. This approach generally results in large particles, which are undesirable for incorporation into composites. Low temperature routes often give access to submicron particles that are well suited for this purpose. The cubic AM_2O_8 phases can be obtained at significantly lower temperatures from a hydroxide hydrate precursor, $AM_2O_7(OH)_2 \cdot 2H_2O$ [21–23]. The transformation proceeds via dehydration to an orthorhombic polymorph [23], which has a similar structure to the cubic phase. The cubic phase forms on further heating to 375–400 °C (molybdates) and 600–650 °C (tungstates), respectively. This kinetically controlled, topotactic recrystallization is the only possible route to the cubic molybdates, which are metastable with respect to their binary oxides and other AMo_2O_8 polymorphs at all temperatures [19,23].

For potential industrial applications, it is important to gain a detailed understanding of the processing variables that affect the crystallization kinetics and resulting particle

*Corresponding author. Fax: +1 419 530 4033.
E-mail addresses: julie.colin@utoledo.edu (J.A. Colin), monty.simon@utoledo.edu (M.D. Simon), kwitker@muskingum.edu (K.L. Witker), cora.lind@utoledo.edu (C. Lind).
[1]Present address: Department of Mechanical Engineering, MS 312, The University of Toledo, Toledo, OH 43606, USA.
[2]Present address: Department of Civil Engineering, MS 307, The University of Toledo, Toledo, OH 43606, USA.
[3]Present address: Department of Chemistry, Muskingum College, New Concord, OH 43762, USA.

0022-4596/$ - see front matter © 2007 Elsevier Inc. All rights reserved.
doi:10.1016/j.jssc.2007.10.012

sizes and shapes of $ZrW_2O_7(OH)_2 \cdot 2H_2O$, the precursor for cubic ZrW_2O_8. For $ZrMo_2O_7(OH)_2 \cdot 2H_2O$, the particle shape can be tuned through the acid choice, giving access to rods, cubes and beams [24]. No studies of crystallization kinetics of $ZrMo_2O_7(OH)_2 \cdot 2H_2O$ have been reported, but the material is equally easily obtained by refluxing in hydrochloric, nitric, or perchloric acid solution. All previously reported syntheses of $ZrW_2O_7(OH)_2 \cdot 2H_2O$ were carried out in hydrochloric acid by reflux or hydrothermal treatments [21,22,25–28]. The reflux method generally yields poorly crystalline samples [22], while hydrothermal synthesis at 170–200 °C results in fast crystallization of high quality $ZrW_2O_7(OH)_2 \cdot 2H_2O$ [27]. It was shown that acid concentration is correlated with particle size and crystallinity [27].

In this paper, we report a detailed study on the crystallization of $ZrW_2O_7(OH)_2 \cdot 2H_2O$ as a function of temperature, acid type, acid concentration, and solution additives. In addition to the previously reported crystalline $ZrW_2O_7(OH)_2 \cdot 2H_2O$ phase, a new zirconium tungstate hydrate phase was observed for some conditions.

2. Experimental

2.1. Materials and methods

All syntheses were carried out in aqueous solutions in air. Reflux and hydrothermal methods were employed. Starting materials were purchased from Alfa Aesar (hydrofluoric, hydriodic and perchloric acid, zirconium oxychloride), Fisher Scientific (hydrochloric, hydrobromic and nitric acid, sodium chloride), and Strem Chemicals (sodium tungstate). Zirconium oxychloride, $ZrOCl_2 \cdot xH_2O$ was dried under vacuum, and stored inside a glove box under argon to keep a constant molecular weight. The effective molecular mass was determined by calcination to ZrO_2, and remained constant over a period of several months ($x \sim 6.8$). For all experiments on crystallization kinetics, liquids were pipetted to ensure accuracy. Parr bomb size, total liquid volume and placement of the bomb in the oven were kept identical to make experiments reproducible. Acid solutions were prepared from concentrated HCl, which was determined to be 13.4 M by titration.

2.2. Synthesis

Reflux and hydrothermal methods were employed. The temperature in the reflux method is limited by the boiling point of the solvent used, while the hydrothermal method can reach higher temperatures by pressurization of the vessel. In a typical synthesis, 1 mmol of $ZrOCl_2 \cdot xH_2O$ and 2 mmol of $Na_2WO_4 \cdot 2H_2O$ were dissolved in 2.00 and 3.00 mL of water, respectively. The two solutions were added to a 23 mL Parr Bomb equipped with a stir bar. A pale yellow precipitate was observed. Then, 5.00 mL of 1.3–13.4 M HCl were added to the Parr bomb. After stirring for approximately 5 min, the bomb was sealed and transferred to a preheated oven at 110–200 °C. Heating times ranged from 1 h to 4 weeks. After cooling, the precipitate was recovered by vacuum filtration through a glass frit. The sample was dried at 60–80 °C, and an off-white to white powder was recovered in 90–95% yield.

2.3. Characterization

Samples were characterized by thermogravimetric/differential thermal analysis (TG/DTA), scanning electron microscopy (SEM) combined with energy dispersive X-ray spectroscopy (EDS), and powder X-ray diffraction (XRD). Thermal analysis data were collected using a TA Instruments SDT 2960 Simultaneous TGA-DTA. Data were collected from 25 to 700 °C in air at a heating rate of 10 °C min^{-1}. SEM and EDS analyses were carried out on a JEOL JSM-6100 microscope. Samples were sputtered with gold before analysis. Ambient temperature XRD data for phase identification were collected on a PANalytical X'Pert Pro diffractometer with an X'Celerator detector. Variable temperature XRD data were collected on a Scintag XDS-2000 diffractometer equipped with a Moxtek detector. Both instruments use Cu$K\alpha$ radiation and Bragg–Brentano geometry. Patterns for phase identification were collected from 5 to 75° 2θ, and variable temperature diffraction patterns were collected over the 5–60° angular range. The temperature was increased from 50 to 750 °C in 50 °C increments. Data were analyzed in JADE [29]. The Crysfire suite [30] was used for indexing.

3. Results and discussion

Crystalline zirconium tungstate hydroxide hydrate can only be obtained in acidic media. Hydrothermal treatment in water yields an amorphous powder, while heating in basic solution results in dissolution of the tungsten species and recovery of tetragonal zirconia.

3.1. Reaction temperature

Only amorphous material was recovered from the reflux method after 4 days in 3.4 M HCl. Broad peaks belonging to $ZrW_2O_7(OH)_2 \cdot 2H_2O$, with some amorphous background, were observed in the powder pattern of a sample refluxed for 7 days in 6.7 M HCl. In contrast, well-crystallized material was obtained in less than a day in a Parr bomb at 170 °C in 3.4 M hydrochloric acid, suggesting that higher temperatures promote the formation of $ZrW_2O_7(OH)_2 \cdot 2H_2O$. All further reactions were carried out in Parr bombs for consistency.

The influence of temperature on the crystallization kinetics of $ZrW_2O_7(OH)_2 \cdot 2H_2O$ was studied for a series of samples prepared in 3.4 M HCl. Reaction temperatures were varied between 110 and 200 °C. An exponential dependence on temperature was observed (Fig. 1).

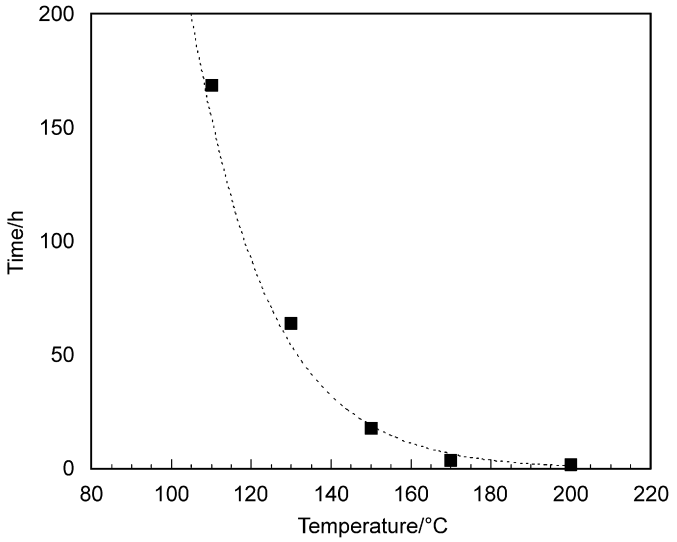

Fig. 1. Temperature dependence of the crystallization of $ZrW_2O_7(OH)_2 \cdot 2H_2O$ in 3.4 M HCl. The indicated times correspond to the shortest treatment that resulted in fully crystallized samples.

3.2. Acid choice

For $ZrMo_2O_7(OH)_2 \cdot 2H_2O$, different particle shapes were reported for experiments carried out in hydrochloric, nitric and perchloric acid [24]. No changes in crystallization kinetics were observed for the three acids. Surprisingly, using the same conditions (3–4 M acid, 170 °C, 3*d*) for the tungstate system, only hydrochloric acid resulted in the formation of crystalline $ZrW_2O_7(OH)_2 \cdot 2H_2O$, while amorphous powders were recovered from HNO_3 and $HClO_4$. Reheating these amorphous powders in 3 M HCl at 170 °C yielded crystalline hydrate. The crystalline phase could also be obtained when NaCl was added to HNO_3 or $HClO_4$ solutions.

According to literature, $ZrW_2O_7(OH)_2 \cdot 2H_2O$ prepared in HCl should be written as $ZrW_2O_7(OH,Cl)_2 \cdot 2H_2O$, as chloride ions can substitute the hydroxy site [22]. Our observations suggested that this substitution was not only possible, but played a crucial role in the crystallization of $ZrW_2O_7(OH,Cl)_2 \cdot 2H_2O$. The presence of chloride in the particles was confirmed by EDS analysis. All crystalline samples prepared in the presence of chloride gave a signal indicating the presence of chlorine. Hydrothermal treatment of a crystalline sample in water decreased the signal for Cl in the EDS below the detection threshold, while XRD confirmed that the crystal structure was preserved. This suggests that the presence of chloride affects the formation of $ZrW_2O_7(OH,Cl)_2 \cdot 2H_2O$, but is not necessary for the stability of the framework once it has crystallized.

3.3. Influence of halides

As the presence of chloride ions facilitated the formation of $ZrW_2O_7(OH,Cl)_2 \cdot 2H_2O$, two studies were conducted to further investigate this effect. In the first study, the identity of the halide ion was varied. Hydrofluoric acid did not produce the hydrate, but resulted in crystallization of sodium zirconium fluoride, $Na_5Zr_2F_{13}$, and tungsten oxide, WO_3. It was found that HBr resulted in crystalline samples. Ideal synthesis conditions were 2–3 M HBr heated at 170 °C for 2 days or longer. Amorphous material was recovered for low (1 M) acid concentrations or lower temperatures (130–150 °C). The liquid phase had a pale brown color after hydrothermal treatment, indicating partial decomposition of HBr to form elemental Br_2. EDS qualitatively confirmed the presence of bromide in the samples. Experiments in HI did not yield crystalline material under any conditions, and the recovered mixtures were dark brown with a strong halogen smell. The inability to form $ZrW_2O_7(OH,X)_2 \cdot 2H_2O$ using hydriodic acid could either be related to the instability of HI at elevated temperatures, or the larger size of I^- compared to Cl^- and Br^-, which prohibits substitution on the hydroxy site.

In a second set of experiments, samples were prepared in 3 M $HClO_4$ at 170 °C with different amounts of chloride ions present. Initial experiments used NaCl as a chloride source and $ZrOCl_2 \cdot xH_2O$ as the zirconium starting material. It was found that lower chloride concentrations required longer heating times. $ZrW_2O_7(OH)_2 \cdot 2H_2O$ can in fact be prepared from $ZrOCl_2 \cdot xH_2O$ in $HClO_4$ without an additional chloride source if the heating time is extended to 5 days ($[Cl^-] = 0.30$ M). In comparison, the same experiment carried out with $ZrO(NO_3)_2 \cdot xH_2O$ as a starting material yields an amorphous product after 7 days at 170 °C, but shows crystalline hydrate after 14 days. This confirms that halide free $ZrW_2O_7(OH)_2 \cdot 2H_2O$ can be prepared.

3.4. Acid concentration

To investigate the effect of hydronium ion concentration on the crystallization kinetics, samples were prepared with different concentrations of perchloric acid at 170 °C. For all reactions, sodium chloride was added to the Parr bombs to obtain reaction mixtures with 3.0 M chloride ion concentration. This step was taken to improve the overall crystallization kinetics. Final acid concentrations varied from 1.5 to 6.0 M. It was found that acid concentration had some influence on the crystallization kinetics, with formation of $ZrW_2O_7(OH)_2 \cdot 2H_2O$ starting between 1.75 h (6.0 M) and 4 h (1.5 M). Fully crystalline $ZrW_2O_7(OH)_2 \cdot 2H_2O$ was recovered after heating for 5 h (4.5–6.0 M) to 7.5 h (1.5–3.0 M).

3.5. Kinetic study in hydrochloric acid

To study the crystallization kinetics in hydrochloric acid, the most commonly used acid for the preparation of $ZrW_2O_7(OH)_2 \cdot 2H_2O$, a series of samples was prepared with hydrochloric acid concentrations between 0.7 and 6.0 M at 170 °C. The precipitates obtained before heat

treatment were amorphous for all acid concentrations. Crystalline $ZrW_2O_7(OH)_2 \cdot 2H_2O$ was observed for all concentrations after sufficient hydrothermal treatment. The crystallization rate increased with acid concentration. For 3.1 M or higher concentrations, the amorphous phase crystallized directly as $ZrW_2O_7(OH)_2 \cdot 2H_2O$. For acid concentrations below 1.5 M, formation of a different polymorph of poor crystallinity was observed at short reaction times. Prolonged hydrothermal treatment resulted in cocrystallization of the new polymorph and $ZrW_2O_7(OH)_2 \cdot 2H_2O$, and finally complete conversion to $ZrW_2O_7(OH)_2 \cdot 2H_2O$. For acid concentrations between 1.5 and 2.7 M, the new polymorph could not be isolated as a pure phase, but the presence of some poorly crystalline new polymorph was evident in samples that already showed crystallization of $ZrW_2O_7(OH)_2 \cdot 2H_2O$ from the amorphous precursor. The new polymorph could not be obtained when only zirconium oxychloride or sodium tungstate were sealed under the same conditions, suggesting that it is a new zirconium tungsten oxide or hydrated polymorph. Thermogravimetric experiments were carried out to address the presence of water. The TGA curve of the new polymorph showed an overall weight loss of ~10%. The major part of the weight loss (8%) occurred in two steps up to 175 °C, with a slower loss and gradual flattening out of the curve up to 400 °C. The total weight loss was of similar magnitude as the one observed for $ZrW_2O_7(OH)_2 \cdot 2H_2O$, which lost 8–10% between 175 and 275 °C (Fig. 2). The weight loss for $ZrW_2O_7(OH)_2 \cdot 2H_2O$ occurred over a much narrower temperature range, which is consistent with a distinct dehydration event leading to a change in crystal structure.

To investigate potential structural changes associated with the dehydration of the new polymorph, an *in situ* variable temperature XRD study was carried out (see Fig. 3). The XRD patterns showed very minor changes between 100 and 150 °C, which may be related to the initial

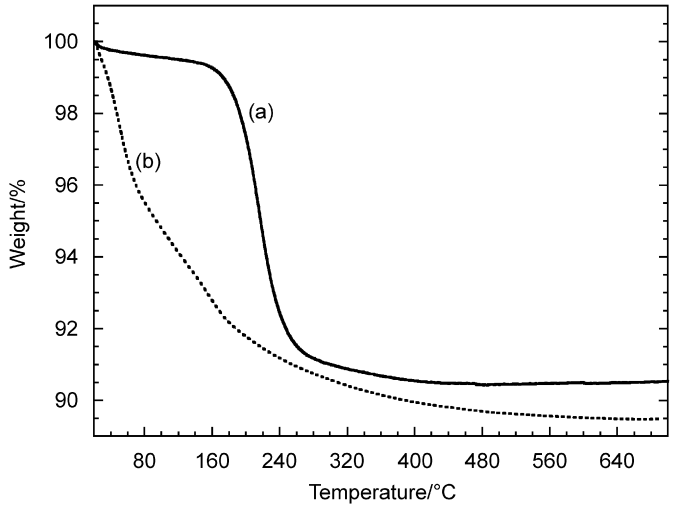

Fig. 2. Thermal analysis data for (a) $ZrW_2O_7(OH)_2 \cdot 2H_2O$ and (b) the new zirconium tungstate hydrate polymorph.

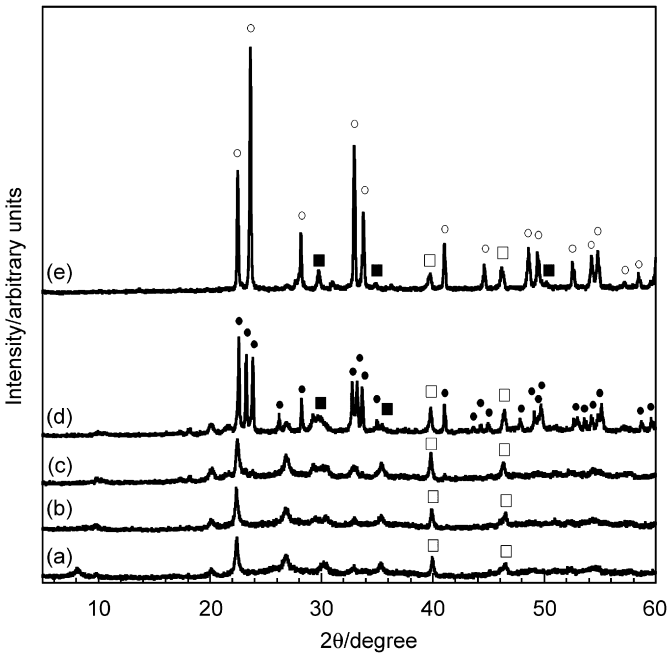

Fig. 3. Variable temperature X-ray diffraction data for $ZrW_2O_8 \cdot xH_2O$ at (a) 50 °C, (b) 150 °C, (c) 550 °C, (d) 600 °C and (e) 700 °C. Peaks corresponding to orthorhombic WO_3 (●), tetragonal WO_3 (○), ZrO_2 (■) and the Pt heater strip (□) are marked.

mass loss. Around 650 °C, crystallization of orthorhombic WO_3 was observed. WO_3 underwent a phase transition between 700 and 750 °C to its tetragonal high temperature structure. At these temperatures, some peaks belonging to cubic or tetragonal ZrO_2 were also observed. To investigate whether the structure observed between 150 and 600 °C could be quenched to ambient conditions, an *ex situ* heat treatment for 2 h at 500 °C was carried out. The sample gave a diffraction pattern that was identical to the *in situ* patterns collected between 150 and 600 °C. This phase is stable during extended heat treatment at 400 °C (50 h), which improved crystallinity slightly (see Fig. 4). TGA on this heat treated sample showed ~3 wt% surface water loss at 100 °C. No similar view cards to either the pattern of the unheated material or the pattern of the 500 °C heated material could be found in the PDF-2 database. Indexing was unsuccessful due to the small number of reliable peaks. While the powder pattern looks simple, many of the peaks are very broad, which could result from overlap of several peaks in a lower symmetry structure. Fig. 5 gives an overview of reaction conditions resulting in amorphous material, crystallization of the new polymorph, $ZrW_2O_7(OH)_2 \cdot 2H_2O$, or a mixture of phases.

3.6. Particle shape

SEM showed that the particle shape was strongly correlated to the crystallinity of the sample. $ZrW_2O_7(OH)_2 \cdot 2H_2O$ crystallizes in a tetragonal structure, which is reflected by the particle shape. For experiments in hydrochloric acid, SEM pictures revealed needle or beam

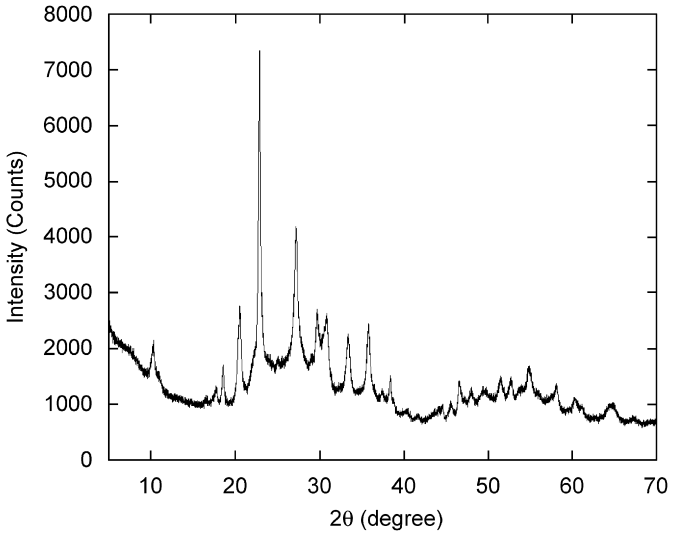

Fig. 4. X-ray diffraction pattern of the new zirconium tungstate polymorph after heat treatment at 500 °C.

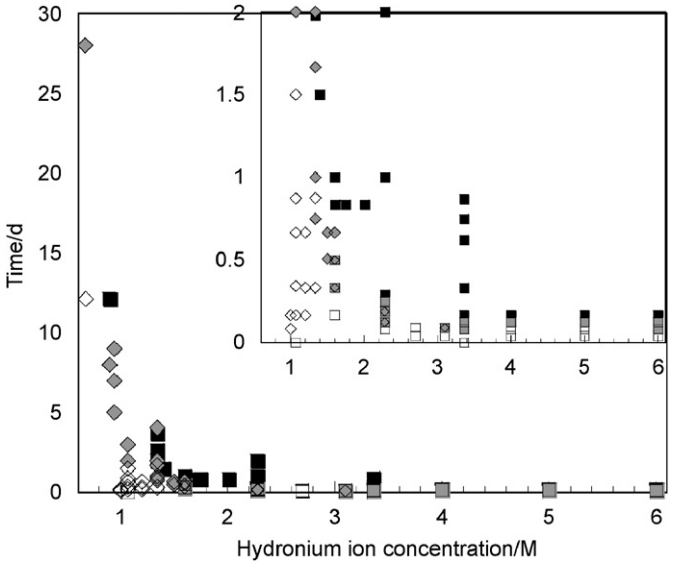

Fig. 5. Phase formation as a function of HCl concentration and reaction time. Experiments yielded amorphous material (□), a mixture of amorphous material and $ZrW_2O_7(OH)_2 \cdot 2H_2O$ (▨), crystalline $ZrW_2O_7(OH)_2 \cdot 2H_2O$ (■),the new zirconium tungstate hydrate polymorph (◇), or a mixture of the new zirconium tungstate hydrate polymorph and $ZrW_2O_7(OH)_2 \cdot 2H_2O$ (◈). The presence of small amounts of the new polymorph in amorphous/$ZrW_2O_7(OH)_2 \cdot 2H_2O$ mixtures is indicated by (▩). A magnified graph for short reaction times is provided as an inset.

like particles with a square cross section, which corresponded to a crystalline PXRD pattern, and agglomerated matter with no specific shape for reaction conditions resulting in amorphous PXRD patterns. The same ill-defined particle shapes were observed for amorphous samples recovered from HNO_3 and $HClO_4$ (Fig. 6). Heat treatment in HNO_3 for 2 weeks again produced beams, correlated to crystalline $ZrW_2O_7(OH)_2 \cdot 2H_2O$. For hydrobromic acid, the correlation between particle shape and

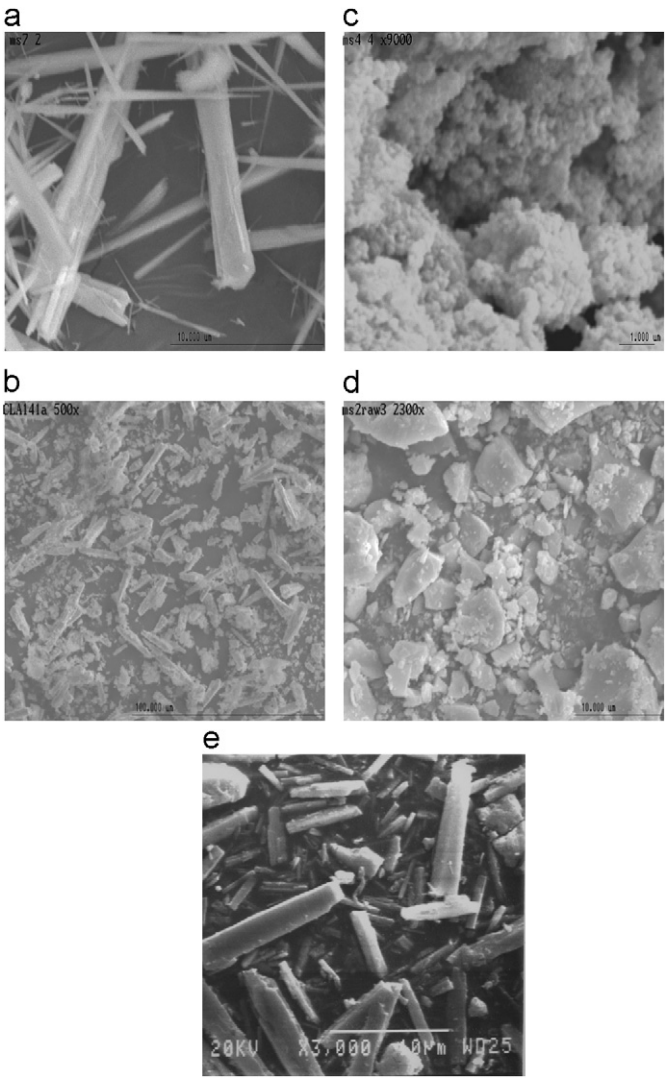

Fig. 6. Particle morphology of samples heated at 170 °C: (a) 3 days in 3 M HCl, (b) 3 days in 3 M HBr, (c) 3 days 3 M HNO_3, (d) 3 days in 3 M $HClO_4$, and (e) 14 days in 3 M $HClO_4$. Samples (a), (b) and (e) correspond to crystalline $ZrW_2O_7(OH)_2 \cdot 2H_2O$, and (c) and (d) display an amorphous X-ray pattern. The scale bars are 10 μm (a), (c), (e), 1 μm (d), and 100 μm (b), respectively.

crystallinity was less obvious. All samples containing crystalline $ZrW_2O_7(OH)_2 \cdot 2H_2O$ showed a mixture of some needlelike particles with large amounts of small, more isotropic particles. No needles were observed in samples that contained no crystalline hydrate. The new phase consisted of agglomerated particles with no particular shape.

4. Conclusions

The formation of $ZrW_2O_7(OH)_2 \cdot 2H_2O$ by hydrothermal synthesis in acidic solutions depends strongly on reaction variables like temperature, acid concentration, and acid type. It was found that chloride ions significantly improve the crystallization kinetics. At high temperatures and hydrochloric acid concentrations, crystallization is

much faster than previously reported conditions. The hydrate phase is fully crystallized after just a few hours at 170 °C for 3.4 M or higher hydrochloric acid concentrations. This shows that careful choice of reaction conditions can significantly reduce the processing time to obtain crystalline $ZrW_2O_7(OH)_2 \cdot 2H_2O$, a precursor to cubic ZrW_2O_8. Crystallization occurs faster in the presence of chloride or bromide ions. Reactions carried out in 3 M $HClO_4$ at 170 °C from chloride free starting materials require 2 weeks to form the hydrate. Using chloride containing starting materials like $ZrOCl_2$ ($[Cl^-] = 0.2$ M), the time for crystallization is reduced by a factor of 2–3. At low acid concentrations, a new, crystalline polymorph is formed initially for acid concentrations below 1.5 M. This new phase is an intermediate for the crystallization of $ZrW_2O_7(OH)_2 \cdot 2H_2O$ at low acid concentrations. For acid concentrations above 3.1 M, formation of $ZrW_2O_7(OH)_2 \cdot 2H_2O$ from an amorphous precursor occurs directly. This is evident from samples recovered from high acid concentrations at shorter reaction times, which contain a mixture of $ZrW_2O_7(OH)_2 \cdot 2H_2O$ and amorphous material, but no new polymorph. Small amounts of the new polymorph are observed in samples of intermediate acid concentrations together with progressive crystallization of $ZrW_2O_7(OH)_2 \cdot 2H_2O$. This suggests that the crystallization kinetics of $ZrW_2O_7(OH)_2 \cdot 2H_2O$ and the new polymorph show very different dependence on acid concentration.

Acknowledgments

This work was supported under National Science Foundation CAREER award DMR-0545517. D.V.C. is grateful for support under the University of Toledo Department of Physics REU program under Grant NSF-REU 0353899, and M.D.S. acknowledges funding through the American Chemical Society's project SEED.

References

[1] A.W. Sleight, Annu. Rev. Mater. Sci. 28 (1998) 29–43.
[2] J.S.O. Evans, J. Chem. Soc. Dalton Trans. (1999) 3317–3326.
[3] A.W. Sleight, Endeavour 19 (1995) 64–68.
[4] J.S.O. Evans, T.A. Mary, A.W. Sleight, Physica B 241 (1997) 311–316.
[5] A.W. Sleight, Inorg. Chem. 37 (1998) 2854–2860.
[6] A.W. Sleight, Curr. Opin. Solid State Mater. Sci. 3 (1998) 128–131.
[7] A. Sleight, Nature 425 (2003) 674–676.
[8] V. Heine, P.R.L. Welche, M.T. Dove, J. Am. Ceram. Soc. 82 (1999) 1793–1802.
[9] M.T. Dove, K.O. Trachenko, M.G. Tucker, D.A. Keen, Rigid unit modes in framework structures: theory, experiment and applications, Transform. Process. Miner. 39 (2000) 1–33.
[10] K. de Buysser, P. Lommens, C. de Meyer, E. Bruneel, S. Hoste, I. Van Driessche, Ceramics-Silikaty 48 (2004) 139–144.
[11] L.M. Sullivan, C.M. Lukehart, Chem. Mater. 17 (2005) 2136–2141.
[12] P. Lommens, C. De Meyer, E. Bruneel, K. De Buysser, I. Van Driessche, S. Hoste, J. Eur. Ceram. Soc. 25 (2005) 3605–3610.
[13] H. Holzer, D.C. Dunand, J. Mater. Res. 14 (1999) 780–789.
[14] D.K. Balch, D.C. Dunand, Metall. Mater. Trans. A 35A (2004) 1159–1165.
[15] C. Verdon, D.C. Dunand, Scr. Mater. 36 (1997) 1075–1080.
[16] T.A. Mary, J.S.O. Evans, T. Vogt, A.W. Sleight, Science 272 (1996) 90–92.
[17] J.S.O. Evans, T.A. Mary, T. Vogt, M.A. Subramanian, A.W. Sleight, Chem. Mater. 8 (1996) 2809–2823.
[18] C. Lind, A.P. Wilkinson, Z.B. Hu, S. Short, J.D. Jorgensen, Chem. Mater. 10 (1998) 2335–2337.
[19] T. Varga, C. Lind, A.P. Wilkinson, H.W. Xu, C.E. Lesher, A. Navrotsky, Chem. Mater. 19 (2007) 468–476.
[20] L.L.Y. Chang, M.G. Scroger, B. Phillips, J. Am. Ceram. Soc. 50 (1967) 211–215.
[21] S.S. Palitsyna, M.V. Mokhosoev, V.I. Krivobok, Bull. Acad. Sci. USSR Div. Chem. Sci. (1977) 611–613.
[22] M.S. Dadachov, R.M.J. Lambrecht, Mater. Chem. 7 (1997) 1867–1870.
[23] S. Allen, N.R. Warmingham, R.K.B. Gover, J.S.O. Evans, Chem. Mater. 15 (2003) 3406–3410.
[24] C. Lind, A.P. Wilkinson, C.J. Rawn, E.A. Payzant, J. Mater. Chem. 11 (2001) 3354–3359.
[25] U. Kameswari, A.W. Sleight, J.S.O. Evans, Int. J. Inorg. Mater. 2 (2000) 333–337.
[26] C. Closmann, A.W. Sleight, J.C. Haygarth, J. Solid State Chem. 139 (1998) 424–426.
[27] X.R. Xing, Q.F. Xing, R.B. Yu, J. Meng, J. Chen, G.R. Liu, Physica B-Condens. Matter 371 (2006) 81–84.
[28] A. Clearfield, R.H. Blessing, J. Inorg. Nucl. Chem. 36 (1974) 1174–1176.
[29] JADE, Materials Data Inc., Livermore, CA, USA, ⟨www.MaterialsData.com⟩.
[30] R. Shirley, The Crysfire 2002 System for Automatic Powder Indexing: User's Manual, The Lattice Press, Guildford, Surrey, England, 2002.